

Interactions between Surfaces in the Presence of Ideal Adsorbing Block Copolymers

J. Ennis* and Bo Jönsson†

Physical Chemistry 2, Chemical Center, P.O. Box 124, S-221 00 Lund, Sweden

Received: August 18, 1998; In Final Form: December 14, 1998

Analytical results are given for the interaction between two planar surfaces separated by a solution of ideal polymers, allowing for a short-range attractive interaction between each monomer and the walls, and treating the cases of both full equilibrium and restricted equilibrium. Results are obtained for a finite chain with discrete monomers, and also for the long chain limit. The behavior of multiblock copolymers is examined by varying the monomer–wall interactions for each monomer.

1. Introduction

Neutral polymers are often used as additives to modify the interactions between colloidal particles. The effect produced is sensitive to the solvent conditions, the polymer volume fraction, and the interactions between the monomers and the particle surfaces. Modern surface force measurements have allowed a more direct investigation of such interactions,^{1–3} and there have been extensive theoretical endeavors to explain the results. In this work the focus is solely on the polymer effect, and other contributions to the force, such as van der Waals interactions, are assumed to be additive.

Some early theories of polymers between surfaces used ideal chains,^{4–7} but more recent research has focused on excluded volume effects and the semidilute regime of concentration, employing a variety of self-consistent mean-field formulations and scaling theories.^{8–12} Most of these works employ a continuous chain model, in which the distribution function for the chain is assumed to satisfy a suitable partial differential equation. This is reasonable if the chains are long enough and the monomer density is not changing too rapidly. Discrete chains, in which the monomers are assumed to be connected by a bonding potential, have generally been studied numerically using lattice models,^{13–15} in which the spatial locations of the monomers are also discretized.

This work reexamines the forces due to ideal adsorbing chains in a slit but extends existing results to encompass the case where each monomer or section of the chain may have a different adsorption strength onto the walls of the slit. Although the assumption of ideality has obvious physical limitations, it should be reasonably close to the Θ temperature, when excluded volume effects are weak, and at low polymer concentration. The major justification for the return to the ideal case is that it allows analytical results to be obtained for quite general distributions of adsorption strengths, and this is a useful reference case for more sophisticated theories or simulations that employ more realistic physical assumptions.

The analysis given in section 2 is in two strands. The first strand involves the solution of the single chain partition function for a discrete ideal chain but with a continuous spatial distribution of monomers, where the strength of the attraction

of each monomer to the wall can be varied independently. This allows the model to treat multiblock copolymers, and it can easily be extended to cover branched polymers and ring polymers. A further application of this solution is in the development of Monte Carlo algorithms for simulating discrete chains in slits, where it is convenient to have an exact solution of a finite discrete ideal chain as a reference case.¹⁶

The second strand of the analysis involves the analytical solution of the long chain limit for the ideal chains under consideration, again allowing for variations in adsorption strengths. It is not at present clear how to obtain the long chain limit directly from the results for the discrete chain, so instead an independent procedure is adopted, which requires the solution of a diffusion equation with a mixed boundary condition. Particularly simple results are obtained in the limit when the adsorbing blocks are strongly adsorbing.

The consistency of the two approaches is demonstrated numerically in section 3, and the homopolymer case is briefly examined. Then results are presented for some multiblock cases, with a focus on ideal telechelic polymers, i.e., polymers with two adsorbing blocks separated by a nonadsorbing block.

2. Model

Discrete Chain. A chain of discrete monomers with a specific bonding potential allows a more detailed consideration of interactions on the monomer scale than is possible with a “continuous” chain, while still being a fairly crude model of a real polymer. It is accessible to simulations and lends itself naturally to lattice models, where it has been studied extensively.¹⁵ However, even in the ideal chain case, there has been limited progress in obtaining analytical results. In the case of an ideal chain adsorbing on a single wall, analytic results in the long chain limit have been obtained directly from the partition function of the discrete chain for quite general bonding potentials.¹⁷ These results confirm that, except in the limit of very strong adsorption, the structure of the adsorbed chain for large N has a universal form that depends only on the number of monomers N , the average monomer–monomer distance a , the adsorption parameter, and the critical adsorption strength.

To obtain the partition function for a single ideal chain between two walls for finite N , a special choice is made for the monomer–monomer potential that is analytically convenient, since the choice of the usual harmonic potential leads to analytical difficulties. In this work, the potential between

* Current address: Research School of Chemistry, Australian National University, ACT 0200, Australia. E-mail: jpek@rsc.anu.edu.au.

† E-mail: bo.jonsson@fkem2.lth.se.

monomers i and $i + 1$ is chosen to be of the form

$$k(|x_{i+1} - x_i| + |y_{i+1} - y_i| + |z_{i+1} - z_i|) \quad (1)$$

where the coordinates of monomer i are given by (x_i, y_i, z_i) . This potential has the peculiar property that the force between the two monomers is constant as their separation increases, although, of course, the energy contribution increases. The properties of an ideal chain of N such monomers become Gaussian as N increases,¹⁸ and as outlined above, the behavior will be independent of the exact form of the bonding potential except on the scale of the monomer–monomer separation.

For the potential given in eq 1 the average monomer–monomer separation a in bulk is given by $a^2 = 6/(\beta k)^2$, where $\beta = 1/(k_B T)$, k_B is Boltzmann's constant, and T is the absolute temperature. The average end to end distance R is given by $R^2 = (N - 1)a^2$ and the radius of gyration R_g by $R_g^2 = (N - 1/N)a^2/6$. The form of potential in eq 1 implies that the chain is not quite spherically symmetric in bulk, but it can be shown that this asymmetry disappears as N^{-1} . For the purpose of computing the pressure between two surfaces, one can in fact generalize slightly to a monomer–monomer potential of the form $u(x_i, x_{i+1}, y_i, y_{i+1}) + k|z_{i+1} - z_i|$ since the integrations over the x and y variables cancel out of the expressions for the pressure.

The interaction of each monomer with the walls is represented by a “sticky” potential.¹⁷ Monomer i is assumed to have some short-range adsorption potential $\psi_i(z)$ at a distance $z \geq 0$ from the wall, and the Boltzmann factor is written as $\exp(-\beta\psi_i(z)) \approx 1 + \bar{W}_i\delta(z)$, where $\delta(z)$ is a one-sided delta function, and $\bar{W}_i = \int_0^\infty (\exp(-\beta\psi_i(z)) - 1) dz$. This should be adequate on length scales greater than the range of the adsorption potential. It is also possible to employ other analytically tractable forms for the adsorption potential, such as combinations of decaying exponentials and powers, albeit at the cost of greater algebraic complexity. This would allow the use of both attractive and repulsive potentials of finite range.

The equitension ensemble is now used to maintain a constant chemical potential in the slit as the width is varied.¹⁶ This shall be referred to as the full equilibrium case. It can be shown that P , the component of the pressure normal to the walls, obeys the relation

$$\frac{P(h_2)}{P(h_1)} = \frac{\partial q}{\partial h} \Big|_{h_2} \Big/ \frac{\partial q}{\partial h} \Big|_{h_1} \quad (2)$$

for wall separations of h_1 and h_2 , where

$$q(h) = \int_0^h \dots \int_0^h \exp(-\beta k \sum_{i=1}^{N-1} |z_{i+1} - z_i|) \times \prod_{i=1}^{N-1} [1 + \bar{W}_i(\delta(z_i) + \delta(z_i - h))] dz_i \quad (3)$$

Surface force measurements indicate that interactions in the presence of strongly adsorbing polymers may take place under nonequilibrium conditions even on a time scale of hours. A crude way of approximating these conditions is to assume that the amount of polymer in the slit is fixed as the separation varies—referred to as “restricted equilibrium”.¹⁴ However, even the more detailed theoretical treatments of uniformly adsorbing chains under restricted equilibrium give only qualitative agreement with experimental data from surface force measurements,¹ with the strength of the attractive forces being underestimated by a factor of 2–3. It may be that a more careful account is

needed of the nonequilibrium nature of the interactions that occur under experimental conditions.

For the canonical system, which corresponds to restricted equilibrium, the pressure is given by

$$\bar{P} = \frac{\partial q}{\partial Z} \Big/ q$$

where $\bar{P} = PR_g/(\sigma k_B T)$, $Z = h/R_g$, and σ is the number of polymer chains in the slit per unit surface area.

The expression for $q(h)$ can be evaluated as

$$q = \frac{1}{(\beta k)^N} \left[2^{N-1} c + 2 \sum_{j=0}^{N-2} b_{N-1,j} \left(j! - e^{-c} \sum_{k=0}^j \frac{c^k j!}{k!} \right) + 2W_N(2^{N-1} + b_{N-1,0} + e^{-c} \sum_{j=0}^{N-2} b_{N-1,j} c^j) \right] \quad (4)$$

where $c = \beta k h$, $W_i = \beta k \bar{W}_i$, and the coefficients $b_{i,j}$ are given by the recurrence

$$b_{i,i-1} = \frac{W_i - 1}{(i - 1)!}$$

$$b_{i,m} = \frac{1}{m} b_{i-1,m-1} + \frac{1}{2} \sum_{j=m}^{i-2} b_{i-1,j} \frac{j!}{2^{j-m} m!} \quad \text{for} \quad 0 < m < i - 1$$

$$b_{i,0} = -2^{i-1} - \frac{1}{2} \sum_{j=0}^{i-2} b_{i-1,j} \left(e^{-c} \sum_{k=0}^j \frac{c^k j!}{2^{j-k} k!} - \frac{j!}{2^j} \right) + W_i(2^{i-1} + b_{i-1,0} + e^{-c} \sum_{j=0}^{i-2} b_{i-1,j} c^j)$$

By differentiating eq 4, one can obtain the following analytic expression for $\partial q/\partial c$:

$$\frac{\partial q}{\partial c} = \frac{1}{(\beta k)^N} \left[2^{N-1} + 2 \sum_{j=0}^{N-2} j! \left(p_{N-1,j} \left(1 - e^{-c} \sum_{k=0}^j \frac{c^k}{k!} \right) + b_{N-1,j} e^{-c} \sum_{k=0}^j \frac{c^k - k c^{k-1}}{k!} \right) + 2W_N(p_{N-1,0} + e^{-c} \sum_{j=0}^{N-2} (b_{N-1,j}(j c^{j-1} - c^j) + p_{N-1,j} c^j)) \right] \quad (5)$$

where $p_{i,j} = \partial b_{i,j}/\partial c$ is given by the recurrence

$$p_{i,i-1} = 0$$

$$p_{i,m} = \frac{1}{m} p_{i-1,m-1} + \frac{1}{2} \sum_{j=m}^{i-2} p_{i-1,j} \frac{j!}{2^{j-m} m!} \quad \text{for} \quad 0 < m < i - 1$$

$$p_{i,0} = -\frac{1}{2} \sum_{j=0}^{i-2} j! \left[p_{i-1,j} \left(e^{-c} \sum_{k=0}^j \frac{c^k}{2^{j-k} k!} - \frac{1}{2^j} \right) + b_{i-1,j} e^{-c} \sum_{k=0}^j \frac{k c^{k-1} - c^k}{2^{j-k} k!} \right] + W_i [p_{i-1,0} + e^{-c} \sum_{j=0}^{i-2} (b_{i-1,j}(j c^{j-1} - c^j) + p_{i-1,j} c^j)]$$

Both recurrences begin with $i = 1$. Since the limiting value of $\partial q/\partial c$ at large separations can be shown to be $2^{N-1}/(\beta k)^N$, eq 2 can be used to obtain P/P_{bulk} where P_{bulk} is the bulk pressure of the polymer solution.

The above results are analytic in the sense that the integrals have been done analytically. The solution for any finite N requires one to evaluate the recurrence relation (since no closed form has yet been obtained), which can easily be handled either by a symbolic algebra program or by a simple piece of code: in both cases one computes all the coefficients of terms involving the scaled variable c , and then evaluates the final expressions for different values of c . The catch is that this requires $O(N^3)$ storage. For large N , these recurrences are best evaluated numerically by fixing the value of c . The computational effort then grows as $O(N^3)$, but only $O(N)$ storage is required, so one can comfortably handle chains of several hundred monomers. To check the long chain limit of this discrete chain case against the analytical results, it is desirable to be able to evaluate the solution for N of $O(10^4)$. For large N the sums in eqs 4 and 5 are dominated by the contributions for $j < 2c$, so for all practical accuracy one need only compute these terms. For separations of the order of R_g , the computational effort is then only $O(N^{5/2})$. A simple Fortran implementation of these procedures is available from the authors.

Other quantities such as the probability distribution for each monomer are readily obtained. The average density of all monomers at a point in the slit requires $O(N^2)$ storage to compute, so in practice is limited to chains of a few hundred monomers in length. Since the focus of this paper is on forces, results for the monomer densities will not be given here.

Long Chain Limit. The probability distribution function G for long chains satisfies a diffusion equation of the following form^{5,18}

$$\frac{\partial G(\mathbf{r}, \mathbf{r}', s, s')}{\partial s} - \frac{a^2}{6} \nabla_{\mathbf{r}}^2 G(\mathbf{r}, \mathbf{r}', s, s') = \delta(\mathbf{r} - \mathbf{r}') \delta(s - s')$$

where \mathbf{r} and \mathbf{r}' are positions in space, s and s' are positions along the chain in number of monomers, and a is again the average monomer–monomer distance of the unconfined chain. This should be valid if the distribution is not changing too rapidly on the scale of the monomer–monomer distance.^{17,19}

For a uniformly nonadsorbing chain in a slit the appropriate boundary condition is $G(\mathbf{r}, \mathbf{r}', s, s') = 0$ on the walls. For a uniformly adsorbing chain, the effect of a short-range adsorption potential can be modeled by a boundary condition of the form¹⁹

$$\frac{\hat{\mathbf{n}} \cdot \nabla_{\mathbf{r}} G}{G} = -\frac{1}{H} \quad (6)$$

where $\hat{\mathbf{n}}$ is the outward normal into the slit and H is an adsorption length. The nonadsorbing case corresponds to $H \rightarrow -\infty$.

These same equations occur in the theory of heat conduction, and analytical solutions in the form of infinite series are available for both the nonadsorbing case and the uniformly adsorbing case.²⁰ These solutions have been used in force calculations (for the nonadsorbing case),^{4–6} as well as in the theory of adsorption chromatography.^{21–23} In the case of adsorption of an ideal chain at an isolated surface, the structure of the adsorbed layer can be obtained from the diffusion equation by an eigenfunction expansion, retaining only the ground state,^{19,24} or the complete

partition function can be obtained by Laplace transforms.^{25,26}

The results for the pressure can be conveniently written in terms of the partition coefficient K , defined as

$$K = \frac{1}{h} \int_0^h dz \int_0^h dz' G(z, z')$$

where $G(z, z')$ gives the probability distribution of the polymer with end points at z and z' (i.e., we have taken $s = 0$ and $s' = N$). The normal component of the pressure at full equilibrium is then given by

$$\frac{P}{P_{\text{bulk}}} = K + Z \frac{dK}{dZ}$$

where Z is again given by $Z = h/R_g$ and in the long chain limit $R_g^2 = a^2 N/6$.

Similarly, at restricted equilibrium the pressure is given by

$$\bar{P} = \frac{1}{Z} + \frac{dZ}{dZ}$$

Now consider an ideal chain made of m different blocks, where block i is characterized by a fixed adsorption length. The probability distribution function of the chain with end points at z_1 and z_{m+1} can then be written as

$$G(z_1, z_{m+1}) = \int_0^h \dots \int_0^h dz_2 \dots dz_m \prod_{i=1}^m G_i(z_i, z_{i+1})$$

where $G_i(z_i, z_{i+1})$ is the distribution function for a uniformly adsorbing chain with adsorption length H_i and a radius of gyration of R_i (where $R_i^2 = a^2 N_i/6$ for a block of length N_i), and end points at z_i and z_{i+1} .

From this one obtains

$$K = 2^m \sum_{i_1=1}^{\infty} \dots \sum_{i_m=1}^{\infty} \exp\left(-\frac{4}{h^2} \sum_{j=1}^m R_j^2 \alpha_{i_j j}^2\right) \lambda_1 \lambda_m \times \prod_{j=1}^m \frac{1}{\lambda_j^2 + \lambda_j + \alpha_{i_j j}^2} \prod_{k=1}^{m-1} \frac{\lambda_k - \lambda_{k+1}}{\alpha_{i_k k}^2 - \alpha_{i_{k+1}, k+1}^2} \prod_{p=2}^{m-1} \alpha_{i_p p}^2 \quad (7)$$

where $\lambda_k = -h/(2H_k)$, and $\alpha_{i_k k}$ is the i_k th root with nonnegative real part of the equation

$$\alpha_{i_k k} \tan(\alpha_{i_k k}) = \lambda_k$$

There is an extensive discussion in Carslaw and Jaeger's book²⁰ of the location of the roots of this equation when $H < 0$. When $H > 0$ the main difference is that there is one purely imaginary root and then a sequence of positive real roots. If a block is nonadsorbing ($\lambda_k \rightarrow -\infty$) then the roots are given by $\alpha_{i_k k} = (2i_k - 1)\pi/2$.

Taking the derivative of K , one obtains

$$\begin{aligned}
Z \frac{dK}{dZ} = & 2^m \sum_{i_1=1}^{\infty} \dots \sum_{i_m=1}^{\infty} \exp \left(-\frac{4}{h^2} \sum_{j=1}^m R_j^2 \alpha_{i_{j,j}}^2 \right) \lambda_1 \lambda_m \times \\
& \prod_{j=1}^m \frac{1}{\lambda_j^2 + \lambda_j + \alpha_{i_{j,j}}^2} \prod_{k=1}^{m-1} \frac{\lambda_k - \lambda_{k+1}}{\alpha_{i_{k,k}}^2 - \alpha_{i_{k+1,k+1}}^2} \times \\
& \prod_{p=2}^{m-1} \alpha_{i_{p,p}}^2 \left[m+1 + \sum_{q=1}^m \frac{1}{\lambda_q^2 + \lambda_q + \alpha_{i_{q,q}}^2} \left(\frac{8}{h^2} R_q^2 \alpha_{i_{q,q}}^2 (\lambda_q^2 + \right. \right. \\
& \left. \left. \alpha_{i_{q,q}}^2) - \left(\lambda_q + 2\lambda_q^2 + 2 \frac{\alpha_{i_{q,q}}^2 \lambda_q}{\lambda_q^2 + \lambda_q + \alpha_{i_{q,q}}^2} \right) \right) - \right. \\
& \left. 2 \sum_{q=1}^{m-1} \frac{1}{\alpha_{i_{q,q}}^2 - \alpha_{i_{q+1,q+1}}^2} \times \right. \\
& \left. \left(\frac{\alpha_{i_{q,q}}^2 \lambda_q}{\lambda_q^2 + \lambda_q + \alpha_{i_{q,q}}^2} - \frac{\alpha_{i_{q+1,q+1}}^2 \lambda_{q+1}}{\lambda_{q+1}^2 + \lambda_{q+1} + \alpha_{i_{q+1,q+1}}^2} \right) + \right. \\
& \left. \left. 2 \sum_{q=2}^{m-1} \frac{\lambda_q}{\lambda_q^2 + \lambda_q + \alpha_{i_{q,q}}^2} \right] \quad (8)
\end{aligned}$$

By combining eqs 7 and 8, one can obtain the pressure at either full or restricted equilibrium. Note at this stage that the behavior of the chain in this limit depends only on two dimensionless parameters for each block, h/H_k and h/R_k , and the sequence of blocks.

To evaluate these expressions, it is necessary to truncate each sum over i_k at n terms, so the sum involves n^m terms. Fortunately, the convergence of the series is sufficiently fast that for typical parameters, $n = 5$ is sufficient to obtain four figure accuracy for $Z < 6$ (for large Z , one can use Laplace transforms to obtain the leading terms in an alternative expansion, but there is no simple closed expression for the general term). If some of the adsorbing blocks have identical properties, then the number of terms in the sum can be further reduced by symmetry. Even so, the computation will soon become impractical as m increases.

A more transparent result can be obtained in the limiting case of a polymer of N monomers with m nonadsorbing blocks of length $n_1 \dots n_m$ monomers, separated and terminated by strongly adsorbing blocks, which can be assumed to lie at one or the other wall (this is less realistic for experiments, since the kinetics of transferring an adsorbed block from one wall to the other would then be very slow, and so equilibrium would be hard to achieve). For each nonadsorbing block, one can then take the solution for a nonadsorbing polymer between two walls and restrict the ends to be very close to the walls (a trick first used for end-adsorbed ideal polymers⁵), allowing for loops (both ends at the same wall) and bridges (ends at different walls). Then at restricted equilibrium the pressure is given by

$$\bar{P} = \sum_{i=1}^m \left(\frac{2\pi^2 r_i \sum_{j=1}^{\infty} (2j-1)^4 \exp(-r_i(\pi(2j-1)/Z)^2)}{Z^3 \sum_{j=1}^{\infty} (2j-1)^2 \exp(-r_i(\pi(2j-1)/Z)^2)} - \frac{3}{Z} \right) \quad (9)$$

where $r_i = R_i^2/R_0^2$. The much simpler structure of the expres-

sions arises from the fact that successive nonadsorbing blocks are effectively independent of one another, because whether one such block forms a loop or a bridge does not depend on the conformation of the other blocks (since all the end points of the blocks lie at the walls).

For small values of Z , one obtains

$$\bar{P} \sim \frac{2\pi^2}{Z^3} - \frac{3m}{Z}$$

Thus the leading term at short range is an entropic repulsion that depends on the combined length of the nonadsorbing blocks, while the next term is attractive and proportional to the number of such blocks.

For large separations ($Z \gg 1$) a more rapidly converging series for the same result is

$$\bar{P} = \sum_{i=1}^m \left(\frac{\sum_{j=1}^{\infty} (-1)^j \exp(-j^2 Z^2/(4r_i)) (j^4 Z^3/(2r_i^2) - 3j^2 Z/r_i)}{1 + \sum_{j=1}^{\infty} (-1)^j \exp(-j^2 Z^2/(4r_i)) (2 - j^2 Z^2/r_i)} \right) \quad (10)$$

For $Z \gg 1$ this gives

$$\bar{P} \sim - \sum_{i=1}^m \exp(-Z^2/(4r_i)) \left(\frac{Z^3}{2r_i^2} - \frac{3Z}{r_i} \right) \quad (11)$$

so the interaction is attractive and dominated by the longest nonadsorbing block(s) (the largest value(s) of r_i).

If in this limiting case the nonadsorbing block at one end (e.g., $i = 1$) is not terminated by a strongly adsorbing block, so there is a tail, then in eq 9 the term for $i = 1$ should be replaced by

$$\frac{2\pi^2 r_1 \sum_{j=1}^{\infty} (2j-1)^2 \exp(-r_1(\pi(2j-1)/Z)^2)}{Z^3 \sum_{j=1}^{\infty} \exp(-r_1(\pi(2j-1)/Z)^2)} - \frac{1}{Z}$$

and in eq 10 by

$$\frac{Z \sum_{j=1}^{\infty} (-1)^{j+1} j^2 \exp(-j^2 Z^2/(4r_1))}{r_1 \left(1 + 2 \sum_{j=1}^{\infty} (-1)^j \exp(-j^2 Z^2/(4r_1)) \right)}$$

In this instance, the pressure at large distances will be repulsive if the longest nonadsorbing block is a tail, and otherwise attractive.

Again, expressions can be derived for the average chain density at a point in the slit, proceeding in the same way from the probability distribution function, but these will not be discussed in this paper.

3. Results

Figure 1 shows the variation of the pressure with separation in the case of nonadsorbing polymers at full equilibrium. This is the classic depletion effect, where the pressure between the

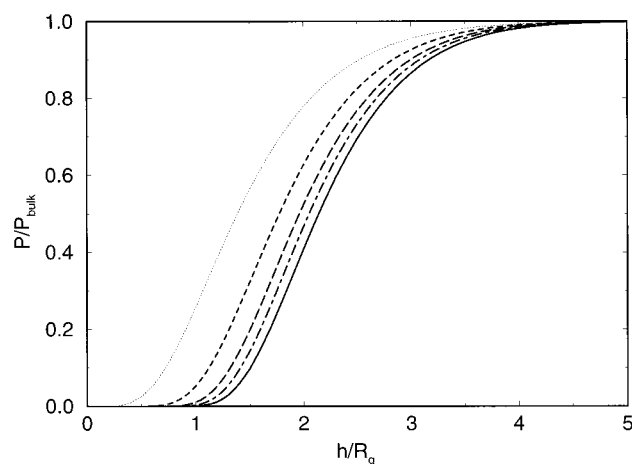


Figure 1. Pressure vs separation for nonadsorbing ideal polymer in equilibrium with bulk: (dotted line) analytic solution for $N = 8$ monomers; (short dashes) $N = 32$; (long dashes) $N = 128$; (dot-dash) $N = 512$; (solid line) long chain limit.

surfaces drops significantly below the bulk pressure at separations less than about $3R_g$, as it becomes entropically unfavorable for the chains to be in the slit, leading to a net attraction. Such a depletion attraction has been observed in recent surface force experiments.³ As N increases, the curves for the discrete monomer case converge as $O(N^{-1/2})$ to the limiting result for long chains, which is⁴

$$\frac{P}{P_{\text{bulk}}} = \frac{8}{\pi^2} \sum_{j=1}^{\infty} \exp(-((2j-1)\pi/Z)^2) \left(\frac{1}{(2j-1)^2} + \frac{2\pi^2}{Z^2} \right)$$

$$= 1 + 4 \sum_{j=1}^{\infty} j(-1)^j \operatorname{erfc}\left(\frac{jZ}{2}\right)$$

where the first form converges best for small Z and the second form for large Z .

In the case of an adsorbing ideal homopolymer, it is well-known that there is a critical value of the adsorption energy per monomer W above which significant adsorption occurs, and which, for very long chains, corresponds to a wetting transition. For the particular monomer–monomer potential employed here, the critical value is $W = 1$, and at this value $\bar{P} = R_g/h$. If one assumes that the monomer–wall interaction is a square well with width equal to a , then this critical value corresponds to an attraction of $0.34 k_B T$ per monomer. Figure 2 shows the effect of varying W for fixed $N = 512$. Here the assumption of restricted equilibrium is employed, which is more realistic for strongly adsorbing polymers ($W > 1$). It can be seen that there is a dramatic change as W is increased beyond the critical value of 1, with the pressure rapidly becoming more attractive at short range. As W is increased further, the range of the attraction decreases, so that at a given separation the pressure increases again.

The analysis for very long chains given in the previous section uses an adsorption length H to characterize the monomer–wall interaction,²³ and in the vicinity of $W = 1$ this is related via¹⁷

$$\frac{a}{H} \approx \sqrt{6} \left(1 - \frac{1}{W} \right) \quad (12)$$

while for large W , $a/H \sim \sqrt{6}(\ln(W))^{1/2}$. From the analytic

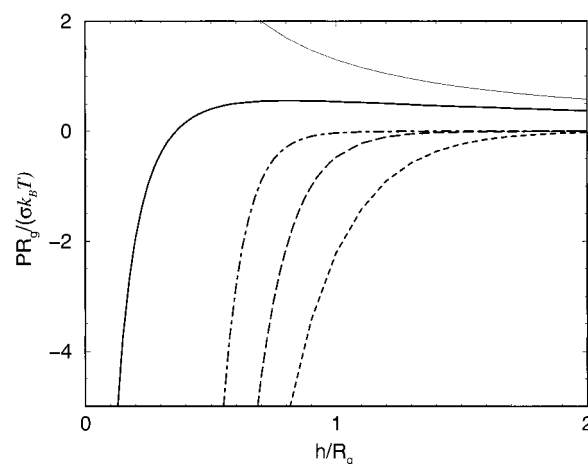


Figure 2. Pressure vs separation for adsorbing ideal polymer at restricted equilibrium, for $N = 512$: (thin solid line) $W = 0.99$; (thick solid line) $W = 1.01$; (short dashes) $W = 1.25$; (long dashes) $W = 1.5$; (dot-dash) $W = 2$.

results in the previous section, it can be shown that for $h/H \gg 1$

$$\bar{P} \approx \frac{2R_g}{H} \left(1 - 2 \left(\frac{R_g}{H} \right)^2 + \frac{h}{H} \right) \exp(-h/H)$$

so that making the chains more adsorbing ($H \rightarrow 0^+$) results in an attraction of larger magnitude but shorter range, as in Figure 2. At short range, the deficiencies of the ideal chain assumption become severe as the monomer density increases. More sophisticated theories²⁷ show that at the Θ temperature, the effect of the third virial coefficient is to make the surface interaction repulsive at short range, which is in qualitative agreement with experiments.

It should be observed that the peculiar nature of the chosen monomer–monomer potential in the discrete chain will show up in these results for ideal uniformly adsorbing chains when the wall separation is of the order of the monomer–monomer separation. Since the force between monomers is constant even at small separations, the pressure between the walls will be attractive all the way to zero separation. If, instead, one uses a harmonic spring, then the force between monomers drops off at small separations, and so the pressure between the walls becomes repulsive at short separations. This can be easily demonstrated by analytically solving the discrete chain case for a two-monomer chain with a harmonic bond. In this same regime the results for the long chain limit predict a uniform attraction, since the model does not take into account the short-range features of the chain. However, these anomalies have no physical importance, since they occur only on a monomer scale, which is not experimentally accessible and where the model is far from realistic.

The approach in this work can be used to treat a wide variety of block copolymers, where the blocks are distinguished on the basis of their interactions with the walls. Consider the case of triblock copolymers with two short adsorbing ends (“stickers”) and a nonadsorbing central block, known as telechelic polymers. This is a prototypical case for more general multiblock copolymers, as will become clear in the succeeding examples. Here the results for the discrete chain will be employed and compared with the limiting case in eq 9. Figure 3 shows the pressure at full equilibrium for telechelic polymers with a central block of length 512 and stickers of various lengths, where each monomer in the sticker blocks has $W = 2$ and the R_g is that of

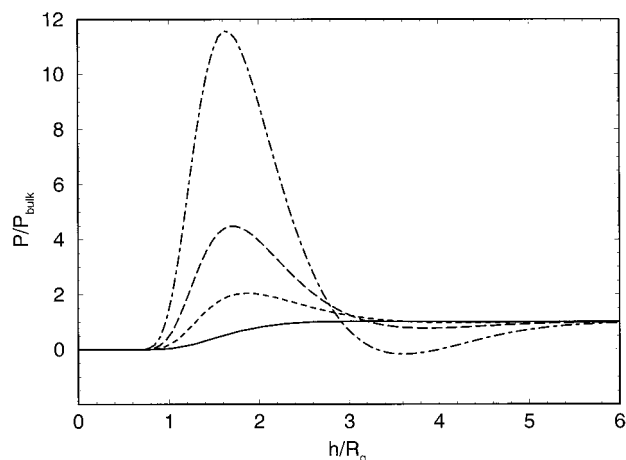


Figure 3. Pressure vs separation for triblock copolymer at full equilibrium. The central block has length 512 monomers, while the N_S monomers in each sticker block have $W = 2$. The R_g used is that of the central block alone. Key: (solid line) $N_S = 10$; (short dashes) $N_S = 14$; (long dashes) $N_S = 16$; (dot-dash) $N_S = 18$.

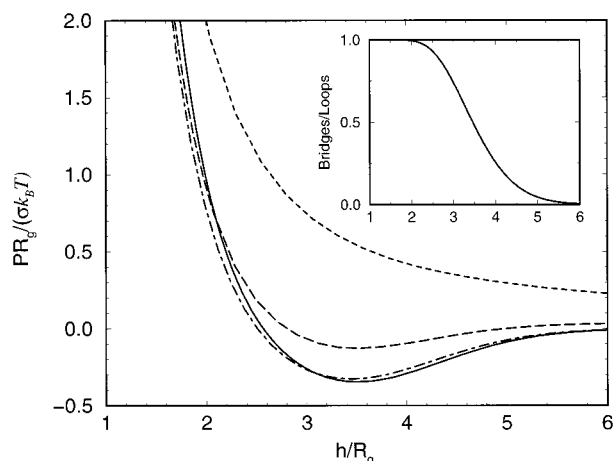


Figure 4. Pressure vs separation for triblock copolymer at restricted equilibrium, parameters as in Figure 3 (apart from N_S): (short dashes) $N_S = 10$; (long dashes) $N_S = 20$; (dot-dash) $N_S = 30$; (solid line) limit for long chains with strong stickers. The inset shows the ratio of the number of bridge conformations to loop conformations in this limit.

the central block alone. If the stickers are shorter than 10 monomers, then the pressure differs only slightly from the pure depletion case. As the sticker length is increased, an attractive minimum appears at larger separations due to bridging, a repulsion appears at a separation of about $1.6R_g$ due to confinement of the nonadsorbing central block, and then at short separations there is a depletion attraction as the chains are squeezed out.

For strongly adsorbing stickers the full equilibrium case becomes unrealistic, first because the ideal nature of the chains leads to large monomer densities in the slit and second because the time required to reach equilibrium may become longer than the time scale of experiments. These deficiencies can be overcome by using restricted equilibrium conditions, as shown in Figure 4. If the stickers are beyond a critical length, then there is again an attractive region in the pressure, with a zero at a separation of about $2.6R_g$, but now the behavior for strong stickers is more reasonable. The analytic solution for long chains with strong stickers is given in eq 9 (or the alternative form in eq 10) for $m = 1$. Note that even when $\bar{P} = 0$, the chain is quite stretched in comparison to its conformation in bulk, the end-to-end distance being larger by about 30%, since the

components of the displacement of the chain in the transverse direction are unaffected by the walls.

The ratio of the number of bridge conformations to the number of loop conformations in this same limit is given by

$$\frac{\text{Pr(bridge)}}{\text{Pr(loop)}} = \frac{\sum_{j=1}^{\infty} (-1)^{j+1} j^2 \exp(-(\pi j/Z)^2)}{\sum_{j=1}^{\infty} j^2 \exp(-(\pi j/Z)^2)}$$

$$= \frac{\sum_{j=1}^{\infty} (Z^2(2j-1)^2 - 2) \exp(-Z^2(2j-1)^2/4)}{1 + \sum_{j=1}^{\infty} (2 - 4j^2 Z^2) \exp(-j^2 Z^2)}$$

where the first form converges rapidly for small Z and the second for large Z . The ratio is plotted in the inset to Figure 4. For separations less than $2R_g$ the ratio is nearly unity, but at larger separation the ratio drops off as the entropic cost of long bridges increases. To leading order, at large distances each bridge contributes $-Z/2$ to the pressure, while the proportion of bridges goes as $Z^2 \exp(-Z^2/4)$. On the other hand, while the proportion of loops approaches 1, each contributes $8Z^3 \exp(-Z^2)$ to the pressure. Thus even a small proportion of bridges is sufficient for the net pressure to be attractive.

Mean-field lattice calculations²⁸ predict a region of attraction qualitatively similar to that in Figure 4. Analysis of the interaction between two polymer brushes of telechelic chains²⁹ predicts a weak attractive minimum in the interaction free energy of strength $k_B T (R_g/h_b)^2$ per chain, where h_b is the height of the isolated brush and $h_b \gg R_g$. As a rough comparison, a layer of ideal telechelic chains on an isolated surface will have a height of order R_g (since the chains do not experience the strong stretching typical of brushes), and the minimum free energy of two interacting layers in the limit of strong adsorption is about $-0.62 k_B T$ at a separation of $2.6R_g$. The interaction of a single brush of telechelic chains with a bare adsorbing surface has also been studied theoretically in a variety of adsorption regimes.³⁰ Since it was assumed that the stickers have affinity only for the bare surface (i.e., there are very few loops formed), it is possible in that analysis for all the chains to bridge, and the attractive minimum can be much deeper than in the case of two interacting brushes.

Surface force experiments with ABA block copolymers under good solvent conditions³¹ show that there can be a region of attraction on the initial approaches between a bare surface and a coated surface, but after a number of cycles this becomes a net repulsion. Recent AFM experiments with hydrophobically modified poly(ethylene oxide) (HM-PEO) on polystyrene surfaces exhibit a similar phenomenon.³² Analysis of the force profile for one of the early approach cycles shows that the maximum attractive force occurs at a separation of around $3R_g$, with a free energy per chain of about $-0.8 k_B T$ per chain and a fitted sticker energy of around $1 k_B T$. Although this force profile does not correspond to equilibrium, it is roughly consistent with the equilibrium predictions made in the current work for ideal telechelic chains.

There is also strong indirect evidence that bridging occurs in systems of telechelic polymers and microemulsions.^{33,34} In the case of HM-PEO in a pentaethylene glycol dodecyl ether—

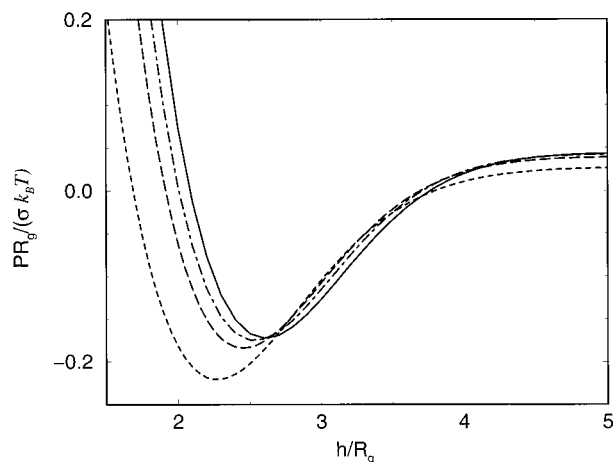


Figure 5. Convergence to the long chain limit for a triblock copolymer at restricted equilibrium: (solid curve) long chain limit for $R_g/H = 3$, $R_s^2/R_g^2 = 0.3$; (short dashes) discrete chain with $N_s = 15$, $N = 50$, $W = 1.7369$; (long dashes) $N_s = 60$, $N = 200$, $W = 1.2692$; (dot-dash) $N_s = 240$, $N = 800$, $W = 1.1187$.

water-decane system,³⁴ when HM-PEO is added to the lamellar phase, there is an initial decrease in interlayer spacing to a minimum, corresponding to about $3R_g$. In the micellar phase, a variety of measurements indicate that a transient network is formed upon addition of HM-PEO, with the proportion of bridges depending upon the droplet concentration. The model adopted here for telechelic polymers assumes that even at restricted equilibrium, the time scale of rearrangement of the stickers is short compared to the time scale of the experiment. If this is not so, then the forces will depend on the conditions under which the samples are prepared.

The convergence of the multiblock discrete chain case to the long chain limit can be checked using the relationship between W and H given in eq 12. Although this is not exact for arbitrary values of W , it has a large enough region of validity around $W = 1$ to be useful. For example, in the case of telechelic polymer with identical stickers, the long chain limit depends on the three dimensionless parameters $Z = h/R_g$, $\gamma = R_g/H$, and the ratio of the block sizes. The goal is to take $N \rightarrow \infty$ in the discrete chain case while keeping Z and γ fixed, and this can be achieved by using $W = 1/(1 - \gamma/\sqrt{N})$, which has the correct limiting behavior (see eq 12 and discussion). Figure 5 shows the convergence to the long chain limit (computed from eqs 7 and 8) for a telechelic polymer with $\gamma = 3$ and $R_s^2/R_g^2 = 0.3$, where R_s is the radius of gyration of one of the stickers. Using this approach the convergence is again $O(N^{1-2})$, and even for quite short chains the qualitative behavior is the same.

For multiblock copolymers, there are obviously a large array of possible distributions for the blocks, including random block copolymers. However, some simplification is afforded by the results given in eqs 9 and 10, which apply to nonadsorbing blocks separated by strongly adsorbing blocks. If all the nonadsorbing blocks are the same size, then at restricted equilibrium the pressure vs separation curve is the same as the solid curve in Figure 4 (the limiting telechelic case) but where the horizontal axis is now h/R_f , where R_f is the radius of gyration of one of the nonadsorbing blocks, and the vertical axis is now $P R_f/(m\sigma k_B)$, where m is the number of nonadsorbing blocks.

This kind of multiblock copolymer can be thought of as another way of modeling an adsorbing polymer, so that rather than every monomer being adsorbing, there are a smaller number of strongly adsorbing monomers spaced along the chain.³⁵ In this case the limiting results indicate that the interaction is



Figure 6. Distribution of blocks of adsorbing monomers (shown in black) for the multiblock copolymer used in Figure 7. The chain has 840 monomers and is divided into blocks as $(A B)_p A$, where the monomers in the A blocks are adsorbing and those in the B blocks are nonadsorbing. Distributions are shown for $p = 1 \dots 6$.

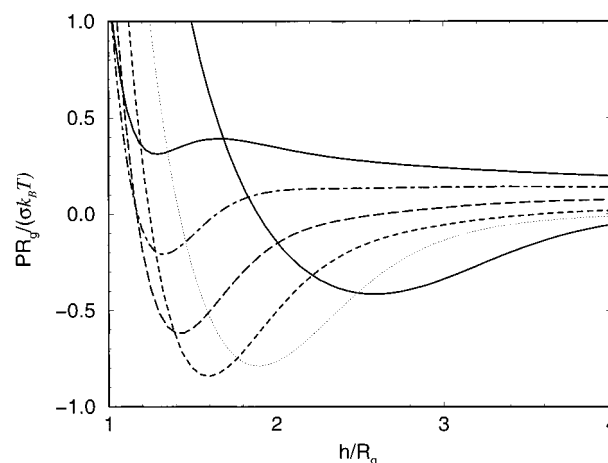


Figure 7. Pressure vs separation for a multiblock copolymer at restricted equilibrium. The chain has 840 monomers and is divided into blocks as $(A B)_p A$, where the monomers in the A blocks have $W = 1.2$, the monomers in each B block have $W = 0$, each A block has $420/(p + 1)$ monomers, and each B block has $420/p$ monomers. See Figure 6 for a schematic of the monomer distribution. Key: (lower solid curve) $p = 1$; (dotted) $p = 2$; (short dashes) $p = 3$; (long dashes) $p = 4$; (dot-dash) $p = 5$; (upper solid curve) $p = 6$.

exponentially small at long range; then there is a strong attractive well at $h \approx 3.5 R_f$, the depth of which scales as $m^{3/2}$ for fixed N . At shorter range ($h < 2.6 R_f$) there is a repulsion, a feature that is absent in the earlier results for the uniformly adsorbing ideal chain (Figure 2).

If the adsorbing blocks in the multiblock copolymer are only weakly adsorbing, then it is possible to have a long-range repulsion as well as an attractive well. Consider a polymer of 840 monomer units, half of which are nonadsorbing and half of which are adsorbing with $W = 1.2$. Now consider block copolymers of the form $(A B)_p A$, where A denotes a block of the adsorbing monomers and B denotes a block of the nonadsorbing monomers. As an aid to the reader, Figure 6 gives a schematic picture of the distribution of the two types of monomers for $p = 1 \dots 6$. Figure 7 shows the results for $p = 1 \dots 6$. For $p = 1, 2$, the length of the adsorbing blocks exceeds the critical block length for $W = 1.2$, and so the pressure roughly follows the form discussed above; e.g., the attractive minimum for $p = 2$ is about twice that for $p = 1$, since p is the number of nonadsorbing blocks. However, for larger values of p , the A blocks are short enough to be only weakly adsorbing, so that while there is still a well at $h \approx 3-4 R_f$, it becomes shallower as p increases, while at large separations there is now a repulsion. Similar behavior is also observed in Scheutjens-Fleer calculations on multiblock copolymers.²⁸ Qualitatively,

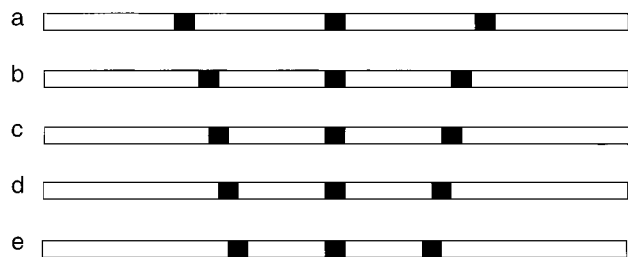


Figure 8. Schematic of the structure of the multiblock copolymers used in Figure 9, with the adsorbing portions of the chain shown in black. The chain has 640 monomers and is divided into blocks as T-A-F-A-F-A-T, where the A blocks have 20 monomers with $W = 4$ and the other monomers have $W = 0$. The lengths of the T and F blocks are denoted N_T and N_F respectively, and $N_F = 270 - N_T$. Key: (a) $N_T = 135$; (b) $N_T = 160$; (c) $N_T = 170$; (d) $N_T = 180$; (e) $N_T = 190$.

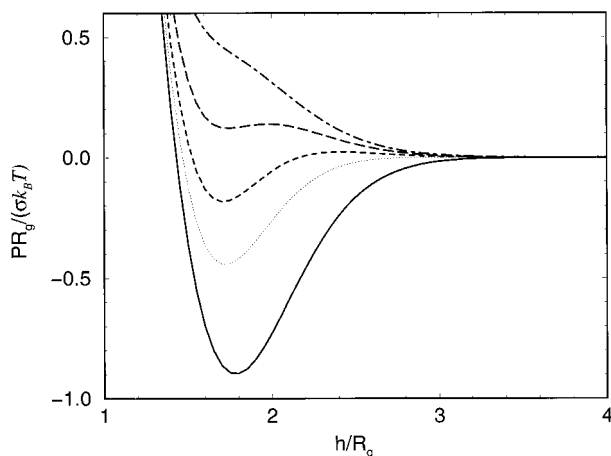


Figure 9. Pressure vs separation for a multiblock copolymer at restricted equilibrium. The chain has 640 monomers and is divided into blocks as T-A-F-A-F-A-T, where the A blocks have 20 monomers with $W = 4$ and the other monomers have $W = 0$. The lengths of the T and F blocks are denoted N_T and N_F , respectively, and $N_F = 270 - N_T$. See Figure 8 for a schematic of the monomer distribution. Key: (solid curve) $N_T = 135$; (dotted) $N_T = 160$; (short dashes) $N_T = 170$; (long dashes) $N_T = 180$; (dot-dash) $N_T = 190$.

one expects that as the number of blocks becomes large, the chain should behave more like a homopolymer with the "average" adsorption strength per monomer. In this case the average is $W = 0.6$ per monomer, and thus the equivalent homopolymer is nonadsorbing.

A similar phenomena occurs for a multiblock copolymer that has a nonadsorbing block at either end, separated by a sequence of strongly adsorbing blocks and nonadsorbing blocks, as deduced from the analysis of the long chain limit in section 2. Then a competition should occur between the tails and the bridges. Consider a discrete chain with 600 monomers. The sequence of blocks is T-A-F-A-F-A-T, where T are the tail blocks of length N_T , A are the adsorbing blocks, and F are the nonadsorbing blocks of length N_F within the chain. The A blocks consist of 20 monomers with $W = 4$, and $N_T + N_F = 270$. A schematic of the arrangement of blocks is given in Figure 8. Figure 9 shows that when $N_T = N_F$, then the pressure is attractive at long-range. As the ratio N_T/N_F increases, the pressure becomes weakly repulsive at long range, and the minimum progressively shallower until it vanishes altogether.

4. Conclusions

An analytic solution has been obtained for the interaction of two surfaces in the presence of ideal polymers, allowing each

monomer or section of the chain to have an attractive interaction with the walls. The analysis has been carried out both for a chain with discrete monomers and for a continuous chain, and the two approaches are shown to agree for long chains. These results give a straightforward way of understanding interactions in the presence of ideal multiblock copolymers.

Some particularly simple formulas are obtained for a sequence of nonadsorbing blocks separated by strongly adsorbing blocks. The pressure at long range is dominated by the longest nonadsorbing block, being attractive if this block has adsorbing blocks on both sides and otherwise repulsive. At separations of the order of the radius of gyration of the nonadsorbing blocks, there may be an attractive minimum (depending on the competition between tails and bridges), and at shorter range there is a repulsion.

Acknowledgment. Thanks to Bo Söderberg for a useful discussion about the monomer-monomer potential.

References and Notes

- (1) Patel, S.; Tirrell, M. *Annu. Rev. Phys. Chem.* **1989**, *40*, 597.
- (2) Biggs, S. *Ber. Bunsen-Ges. Phys. Chem.* **1994**, *98*, 636.
- (3) Ruths, M.; Yoshizawa, H.; Fetters, L. J.; Israelachvili, J. N. *Macromolecules* **1996**, *29*, 7193.
- (4) Asakura, S.; Oosawa, F. *J. Chem. Phys.* **1954**, *22*, 1255.
- (5) Dolan, A. K.; Edwards, S. F. *Proc. R. Soc. London, Ser. A* **1974**, *337*, 509.
- (6) Richmond, P.; Lal, M. *Chem. Phys. Lett.* **1974**, *24*, 594.
- (7) Vrij, A. *Pure Appl. Chem.* **1976**, *48*, 471.
- (8) Dolan, A. K.; Edwards, S. F. *Proc. R. Soc. London, Ser. A* **1975**, *343*, 427.
- (9) Joanny, J. F.; Leibler, L.; de Gennes, P. G. *J. Polym. Sci., Polym. Phys. Ed.* **1979**, *17*, 1073.
- (10) de Gennes, P.-G. *Macromolecules* **1982**, *15*, 492.
- (11) de Gennes, P. G. *Adv. Colloid Interface Sci.* **1987**, *27*, 189.
- (12) Semenov, A. N.; Joanny, J. F.; Johnner, A.; Bonet-Avalos, J. *Macromolecules* **1997**, *30*, 1479.
- (13) DiMarzio, E. A.; Rubin, R. J. *J. Chem. Phys.* **1971**, *55*, 4318.
- (14) Scheutjens, J. M. H. M.; Fleer, G. J. *Macromolecules* **1985**, *18*, 1882.
- (15) Fleer, G. J.; Cohen Stuart, M. A.; Scheutjens, J. M. H. M.; Cosgrove, T.; Vincent, B. *Polymers at Interfaces*; Chapman and Hall: London, 1994.
- (16) Svensson, B.; Woodward, C. E. *Mol. Phys.* **1996**, *87*, 1363.
- (17) Chan, D.; Mitchell, D. J.; Ninham, B. W.; White, L. R. *J. Chem. Soc., Faraday Trans. 2* **1975**, *71*, 235.
- (18) Chandrasekhar, S. *Rev. Mod. Phys.* **1943**, *15*, 1.
- (19) de Gennes, P. G. *Rep. Prog. Phys.* **1969**, *32*, 187.
- (20) Carslaw, H. S.; Jaeger, J. C. *Conduction of Heat in Solids*, 2nd ed.; Oxford University Press: Oxford, U.K., 1959.
- (21) Casassa, E. F. *J. Polym. Sci. B* **1967**, *5*, 773.
- (22) Skvortsov, A. M.; Gorbunov, A. A. *J. Chromatogr.* **1980**, *358*, 77.
- (23) Gorbunov, A. A.; Skvortsov, A. M. *Adv. Colloid Interface Sci.* **1995**, *62*, 31.
- (24) Jones, I. S.; Richmond, P. J. *J. Chem. Soc., Faraday Trans. 2* **1977**, *73*, 1062.
- (25) Lépine, Y.; Caillé, A. *Can. J. Phys.* **1978**, *56*, 403.
- (26) Eisenriegler, E.; Kremer, K.; Binder, K. *J. Chem. Phys.* **1982**, *77*, 6296.
- (27) Ingersent, K.; Klein, J.; Pincus, P. *Macromolecules* **1990**, *23*, 548.
- (28) Wijmans, C. M.; Leermakers, F. A. M.; Fleer, G. J. *J. Colloid Interface Sci.* **1994**, *167*, 124.
- (29) Milner, S. T.; Witten, T. A. *Macromolecules* **1992**, *25*, 5495.
- (30) Johnner, A.; Joanny, J.-F. *J. Chem. Phys.* **1992**, *96*, 6257.
- (31) Dai, L.; Toprakcioglu, C. *Macromolecules* **1992**, *25*, 6000.
- (32) Courvoisier, A.; Isel, F.; François, J.; Maaloum, M. *Langmuir* **1998**, *14*, 3727.
- (33) Quellet, C.; Eicke, H.-F.; Xu, G.; Hauger, Y. *Macromolecules* **1990**, *23*, 3347.
- (34) Bagger-Jørgensen, H.; Coppola, L.; Thuresson, K.; Olsson, U.; Mortensen, K. *Langmuir* **1997**, *13*, 4204.
- (35) Marques, C. M.; Joanny, J. F. *Macromolecules* **1990**, *23*, 268.